



## Discrete element modeling of explosion-induced fracture extension in jointed rock masses

M. Lak<sup>1</sup>, M. Fatehi Marji<sup>1\*</sup>, A.R. Yarahmadi Bafghi<sup>1</sup> and A. Abdollahipour<sup>2</sup>

1. Faculty of Mining and Metallurgical Engineering, Yazd University, Yazd, Iran

2. Drilling & Well Completion Technologies & Research Group, Research Institute of Petroleum Industry (RIPI), Tehran, Iran

Received 23 July 2018; received in revised form 27 November 2018; accepted 29 November 2018

### Keywords

*Rock Mass Explosion*

*Dynamic Fracturing*

*Crack Extension*

*Discrete Element Method*

*Discrete Fracture Network*

### Abstract

The explosion process of explosives in a borehole applies a very high pressure on its surrounding rock media. This process can initiate and propagate rock fractures, and finally, may result in the rock fragmentation. Rock fragmentation is mainly caused by the propagation of inherent pre-existing fractures of the rock mass and also from the extension of the newly formed cracks within the intact rock due to the explosion. In this work, the process of extension of blast-induced fractures in rock masses is simulated using the discrete element method. It should be noted that, in this work, fracture propagation from both the rock mass inherent fractures and newly induced cracks are considered. The rock mass inherent fractures are generated using the discrete fracture network technique. In order to provide the possibility of fracture extension in the intact rock blocks, they are divided into secondary blocks using the Voronoi tessellation technique. When the modeling is completed, the fracture extension processes in the radial and longitudinal sections of a borehole are specified. Then a blast hole in an assumed rock slope is modeled and the effect of pre-splitting at the back of the blast hole (controlled blasting) on the fracture extension process in the blast area is investigated as an application of the proposed approach. The modeling results obtained show that the deployed procedure is capable of modeling the explosion process and different fracture propagations and fragmentation processes in the rock masses such as controlled blasting.

### 1. Introduction

The excavation of rocks by means of blasting is usually established by breaking the rocks into smaller pieces and creating various surface and underground structures in most mining and civil engineering projects. The dynamic fracture of rocks due to explosion mainly occurs due to stress wave propagation (within the rock) in a very short time (milliseconds). Some applications of the explosion-induced fractures are in mine blasting with the aim of rock fragmentation [1-3] and controlled blasting in civil engineering activities for rock excavation with a minimum damage to the remaining parts of the rock. Mechanical behaviors of rocks affected by high explosion loads are difficult and costly to be studied

exclusively by the instrumentation and experimental works. Therefore, the investigation of rock dynamic fracture mechanisms can be studied promptly by the sophisticated numerical methods [4, 5]. Numerical modeling of these phenomena can also help to gain more information about the explosion and fragmentation process of rocks.

Numerical modeling of rock blasting and numerical investigation of crack extension around the blast hole have been considered by some researchers in the past. The crack propagation problem from the tips of two and more radial cracks around a blast hole has been solved using the displacement discontinuity method in a

✉ Corresponding author: [mfatehi@yazd.ac.ir](mailto:mfatehi@yazd.ac.ir) (M. Fatehi Marji).

quasi-static manner [6-8]. The dynamic studies have also been performed using different numerical methods with different aims such as the investigation of crack propagation patterns around the blast hole in small [9-13] and large scales [14-16]. The effects of the free face *in situ* stresses and load density on the rock fracturing process have been investigated by several researchers [17-20]. Some of these studies have also been conducted by comparing the numerical and physical modeling of fracture extension due to rock explosion [21, 22]. Analytical [23, 24] and numerical [25] modeling of blast-induced wave propagation in rocks and comparison of the results with those for field measurements [26, 27] have also been the subjects of some studies.

It should be noticed that in the above-mentioned approaches, the rock mass was considered as a continuum material. However, the rock masses that are exposed to explosion load may contain naturally pre-existing fractures. The response of these fractures to time-dependent loads is different from that of constant static loads [28, 29]. There are some studies conducted already by some researches who investigated the effect of a pre-existing crack [12, 30] or a fault [31] near a blast hole on the crack propagation around it after detonation.

There are two events caused by blasting in the rock masses: inherent fractures of the rock mass propagation and split due to the explosion. In addition, the intact rock breaks and some new cracks are created within. In this work, a discrete element modeling of fracture propagation in rock mass around a blast hole was performed using the dual fracture media approach. It should be noted that previously the dual fracture media approach was utilized for the simulation of fluid flow modeling in dual porous media (rock masses) [32, 33]. In this approach, the discrete fracture network (DFN) is used for simulation of the pre-existing fractures in rock masses. The Voronoi tessellation technique has also been used for dividing the rocks into secondary blocks in order to provide the possibility of fracture propagation in intact rock blocks. In this case, the explosion-induced fracture propagation is simulated considering both the pre-existing fractures and the newly created cracks in the intact rock. Moreover, the geomechanical properties of the Voronoi sub-blocks and contacts between them have been set in order to close their mechanical behavior to the intact rock behavior. Therefore, crack initiation and propagation in the intact rock around the blast hole can also occur.

## 2. Theoretical background and basic assumptions

The distinct element method (DEM) is basically an explicit finite difference numerical technique that is commonly used for stability assessment, and failure and deformation of discontinuous media. After being proposed by Cundall [34], the method was widely used to model discontinuous jointed rocks in geomechanics. In this work, a 2D distinct element method was used to model the fractured rock mass under dynamic loading conditions. In this approach, the intact rock blocks can have linear or non-linear elastoplastic behaviors individually. The discontinuity motions are governed by the linear or non-linear force-displacement behaviors in normal and shear directions [35]. These governing equations are the Cauchy equations of motion for deformable bodies and various constitutive equations of the rock matrix and fractures [36]. In the present work, the intact rock blocks were simulated by the Mohr-Coulomb plastic constitutive model, and the Coulomb slip model (area contact) was also applied to consider the behavior of rock joints.

As shown in Figure 1, for the elastic rock joints, the stress-displacement incremental relation in the normal direction is assumed to be linear and governed by the stiffness  $k_n$  such that:

$$\Delta\sigma_n = -k_n \Delta u_n \quad (1)$$

where  $\Delta\sigma_n$  is the effective normal stress increment and  $\Delta u_n$  is the normal displacement increment. Also there is a limiting tensile strength,  $\sigma_t$ , for the joints. If the tensile strength exceeds (i.e.  $\sigma_n < -\sigma_t$ ),  $\sigma_n = 0$ . In the shear direction, the response is similarly controlled by a constant shear stiffness  $k_s$ . The shear stress,  $\tau_s$ , is limited by a combination of cohesive ( $C$ ) and frictional ( $\phi$ ) strengths. Therefore, if:

$$|\tau_s| \leq c + \sigma_n \tan \phi = \tau_{\max} \quad (2)$$

then:

$$\Delta\tau_s = -k_s \Delta u_s^e \quad (3)$$

or if:

$$|\tau_s| > \tau_{\max} \quad (4)$$

then:

$$\tau_s = -\text{sign}(\Delta u_s) \tau_{\max} \quad (5)$$

where  $\Delta u_s^e$  is the elastic component of the incremental shear displacement and  $\Delta u_s$  is the total incremental shear displacement [20, 37].

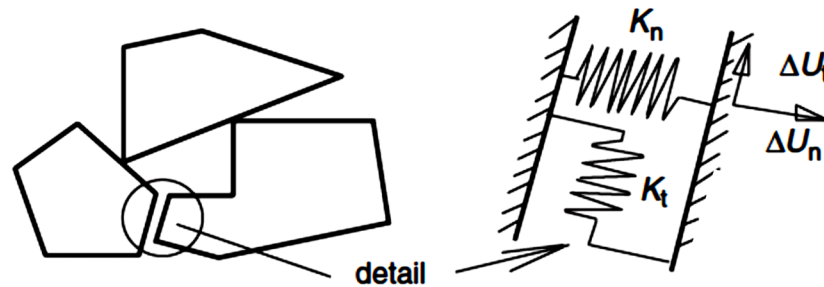


Figure 1. The normal and shear behaviors of the joints [36].

### 3. Modeling strategy

As mentioned earlier, the discrete element method is utilized to model the blast-induced fracture extension using the dual fracture media approach. The first stage of the numerical modeling is to model geometry construction. In this work, Discrete Fracture Network (DFN) was used to model inherent cracks of the rock mass, and the Voronoi tessellation technique was used to model fracture propagation in intact rock blocks. Identifying the geomechanical properties of the intact rock and rock fractures was performed at the next stage. After assignment of the geometrical and geomechanical properties to the rock medium, dynamic modeling was started. At this stage, the dynamic input pulse, damping of the model, element size, and viscous boundaries were important issues. Then the results of the modeling were presented, and a typical example of controlled blasting was performed as an application of the proposed approach.

### 4. Model geometry of a blast hole in a jointed rock mass

In the present work, two radial and longitudinal sections of a blast hole were considered. The dimensions of the radial and longitudinal sections were  $5 \times 5$  m and  $5 \times 10$  m, respectively, and radius of the blast hole was 0.05 m. As mentioned earlier, in order to bring the rock mass fracture system closer to reality, and, on the other hand, to make possible the fracture extension in the intact rock blocks, the dual fracture media approach of the rock is utilized for geometric simulation of

discontinuities. In this approach, the stochastic discrete fracture network (DFN) modeling, assuming that geometrical parameters of the fractures are statistically distributed into the rock mass pre-existing fractures, the Voronoi tessellation technique is used in the intact rock blocks. The geometrical parameters of DFN generation are tabulated in Table 1. In the Voronoi tessellation technique, the intact rock blocks were sub-divided into Voronoi sub-blocks with arbitrary sizes [35]. It should be noted that the fracture system data for generation of DFN in this work are taken from the result of field investigation at the northern slope of Choghart iron mine in Yazd (Iran). Figure 2 shows the geometry and dimensions of the modeling.

### 5. Geomechanical properties of the numerical modelling

As mentioned earlier, the Voronoi tessellation was used in this work to sub-divide the intact rock blocks into the secondary blocks. However, it should be noted that the contacts between the secondary blocks (which are considered as a type of joints in reality) do not actually exist, and they are generated here artificially to model the explosion-induced fracture extension in the intact rock. The physical and mechanical characteristics of the Choghart iron mine have resulted from several laboratory tests such as unconfined and confined compressive pressure tests. Table 2 shows the geomechanical properties of the intact rock and joints of the northern slope of the Choghart iron mine.

Table 1. Geometrical parameters of DFN generation.

Parameters	Dip (°)		Dip direction (°)		Spacing (m)		Trace length (m)		Fisher constants
	M*	SD**	M	SD	M	SD	M	SD	
Js1	70.55	3.312	220.85	6.87	2.461	0.206	11.537	1.782	44
Js2	74.449	6.749	314.84	8.6	0.627	0.433	19.566	2.568	24
Js3	35.354	9.01	23.114	6.867	0.739	0.434	7.44	1.32	35

\* Mean

\*\* Standard Deviation

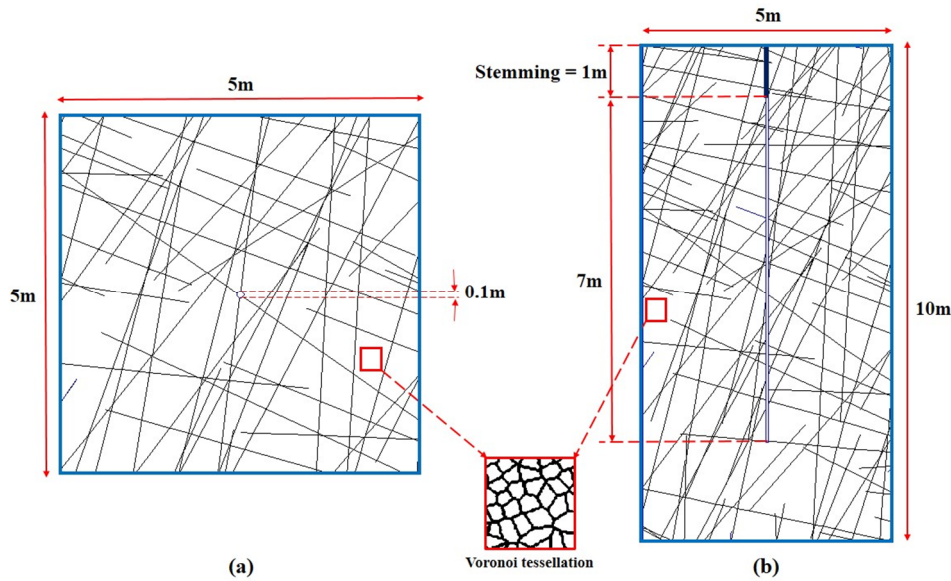


Figure 2. Total geometry of a) radial and b) longitudinal DFN models.

Table 2. Geomechanical properties of intact rock and rock joints of the northern slope [38].

Intact rock	Density (kg/m <sup>3</sup> )	Bulk modulus (GPa)	Shear modulus (GPa)	Cohesion (MPa)	Friction angle (°)
	2603	18	13	27.6	41.8
Rock joints	Normal stiffness (GPa/m)		Shear stiffness (GPa/m)	Cohesion (MPa)	Friction angle (°)
	150.2		75	0.262	32.2

The geomechanical properties of these contacts are naturally governed by contacts between the grains, crystals, minerals, and other small components of the intact rock. In this work, an especial type of calibration is proposed to acquire the geomechanical properties of these secondary contacts. In this calibration, a uniaxial compressive strength test was numerically simulated on a sample of intact rock, which was sub-divided by Voronoi tessellation. This

numerical test was repeated for several times by introducing new property sets for Voronoi sub-block contacts at each time, and the results of rock behaviors were compared with those for the original intact rock (not sub-divided by Voronoi tessellation). Finally, the properties of the best curve-fit behavior were selected. Figure 3 displays the diagram of Voronoi model behavior and a simple (without Voronoi tessellation) specimen.

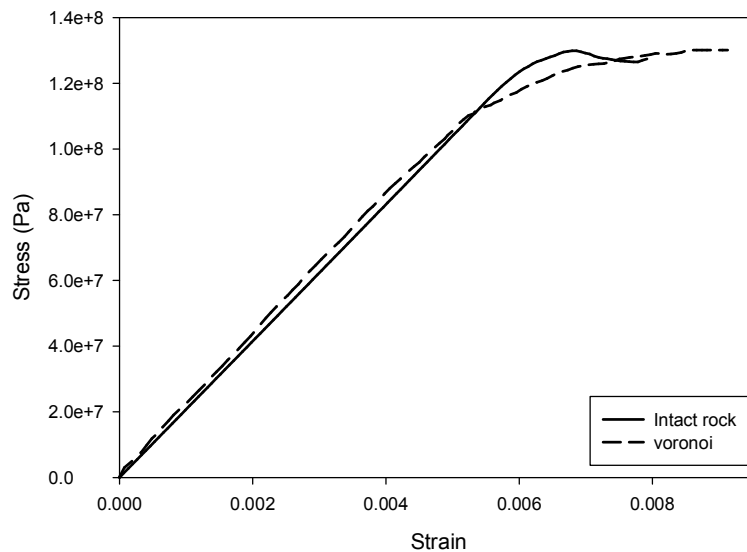


Figure 3. Stress-strain behavior of the sample with and without Voronoi.

### 6. Dynamic modelling of explosion process

Dynamic analysis is often very complicated and requires a considerable amount of insight to be correctly interpreted. These analyses are required for problems involving high frequency and short duration loads like that of seismic or explosion, in which the full dynamic equations of motion (including inertial terms) are solved and the generation and dissipation of kinetic energy directly affect their solutions [35].

All rock blocks considered in the present work were assumed to be deformable. These deformable blocks were composed of finite-difference zones and mechanical changes (e.g. stress/strain), which were calculated within each zone. In the dynamic analysis of rock blocks, the size of an element (or sizes of finite difference zones) should be regarded so that the waves are truly transmitted and they cannot make any

numerical distortion. To this end, the natural frequency of the system and the pre-dominant frequency of the input waves were obtained as well. One of the methods available for obtaining the natural frequency is model release under its own weight without damping. Under these circumstances, the system begins to vibrate, and due to the lack of damping, the vibrations will not stop. In this case, natural frequency can be obtained by counting oscillations in one second. Oscillations of the natural frequency of our case study were 270 Hz. Moreover, the Fast Fourier Transform (FFT) on the acceleration of input waves was deployed to acquire the pre-dominant frequency [35]. Hence, the maximum Fourier amplitude of the input waves, as shown in Figure 4, occurred at a frequency of 2213 Hz. The special element size must be smaller than approximately one-tenth to one-eighth of the wavelength.

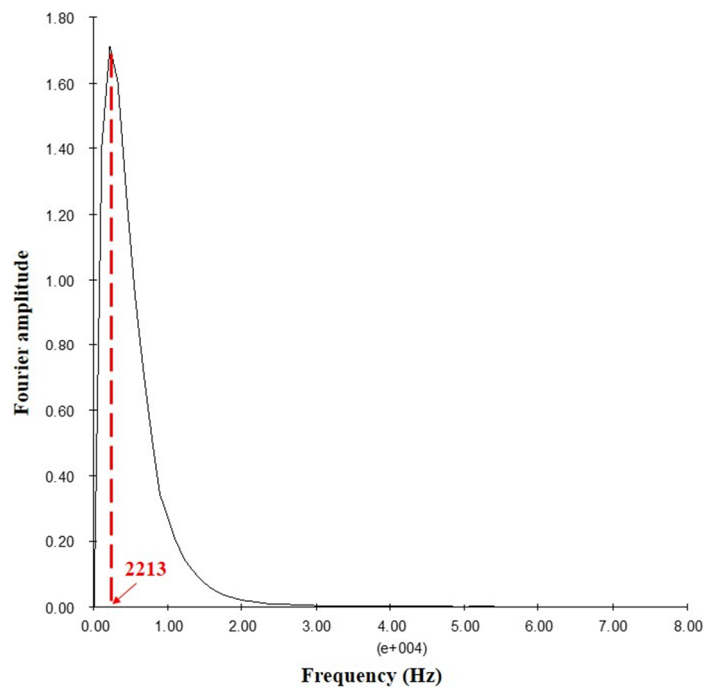


Figure 4. Frequency content of input wave.

The most important stage of a dynamic analysis is the dynamic input of the system. In the present work, the explosion-induced pressure pulse was a detonation by Ammonium Nitrate-Fuel Oil (ANFO) with a density of 0.8 g/cm<sup>3</sup> and a detonation velocity of 2400 m/s. There were several equations available to calculate the pressure of detonation ( $P_d$ ) [39, 40]. Based on [40], the detonation pressure of an explosive depends upon its ingredients (apart from the density and the detonation velocity). This parameter can be estimated using the following equation:

$$P_d = 432 \times 10^{-6} \times \rho_e \times \frac{V_d^2}{1 + (0.8\rho_e)} \quad (6)$$

where  $P_d$  is the pressure of detonation in MPa,  $\rho_e$  is the explosive density in g/cm<sup>3</sup>, and  $V_d$  is the velocity of detonation in m/s [40].

Moreover, the variations in the borehole wall pressure with time lapse ( $P(t)$ ) is significant as a result of the explosion. Many of the past studies have proposed functions to obtain  $P(t)$  such as [2, 9, 10]. The most important solution for the stress distribution around a spherical explosive source

has already been derived [41]. The transient spherical cavity pressure is represented by the following expression [42]:

$$P = P_0 e^{-\alpha t} \quad (7)$$

where  $P_0$  is the peak wall pressure and  $\alpha$  is a positive frequency-dependent decay constant. An elaboration of the Sharpe solution by [23] was based on the assumption that the cavity pressure could be represented by the expression:

$$P = P_0 (e^{-\alpha t} - e^{-\beta t}) \quad (8)$$

since this is merely the superposition of two separate temporal pressure variations with the decay constant  $\beta$  [42]. The transient borehole pressure for the long column of explosive is similarly derived as:

$$P = P_0 \xi (e^{-\alpha t} - e^{-\beta t}) \quad (9)$$

where  $\xi$  is a variable representing the rising and decaying phases of the pressure pulse and  $t_0$  is the time required to achieve the peak pressure. They are obtained by [9, 17]:

$$\xi = 1 / (e^{-\alpha t_0} - e^{-\beta t_0}) \quad (10)$$

$$t_0 = (1 / (\alpha - \beta)) \cdot \log(\beta / \alpha) \quad (11)$$

The decay constants  $\alpha$  and  $\beta$  in the above equations can be achieved by:

$$\alpha = \omega / 4\sqrt{2} \quad (12)$$

$$\beta = \omega / 2\sqrt{2} \quad (13)$$

$$\omega = \frac{2\sqrt{2}C_p}{3a} \quad (14)$$

$$C_p = \sqrt{\frac{K + \left(\frac{4G}{3}\right)}{\rho_r}} \quad (15)$$

where  $C_p$  is the P-wave velocity in the rock media,  $a$  is the borehole radius,  $K$  is the bulk modulus of the rock medium,  $G$  is the shear modulus of the rock medium, and  $\rho_r$  is the rock density [2, 23]. Consequently, the input pressure pulse in this work was achieved as that shown in Figure 5.

In dynamic problems, any of the unreal boundaries cause the created waves to go back into the medium after reaching these boundaries. The solution scheme for this problem involves dashpots attached independently to the boundary in the normal and shear directions [43]. The dashpots provide viscous normal and viscous shear tractions, given by:

$$t_n = -rC_p v_n \quad (16)$$

$$t_s = -rC_s v_s \quad (17)$$

$$C_s = \sqrt{\frac{G}{\rho_r}} \quad (18)$$

where  $v_n$  and  $v_s$  are the normal and shear components of the velocity at the boundary, and  $C_p$  and  $C_s$  are the P- and S-wave velocities that can be obtained from Equations 15 and 18, respectively [26, 44]. Thus the rock external boundaries impose non-reflection conditions so that the stress wave could transmit away from the boundaries and would not reflect on the rock medium (Figure 6).

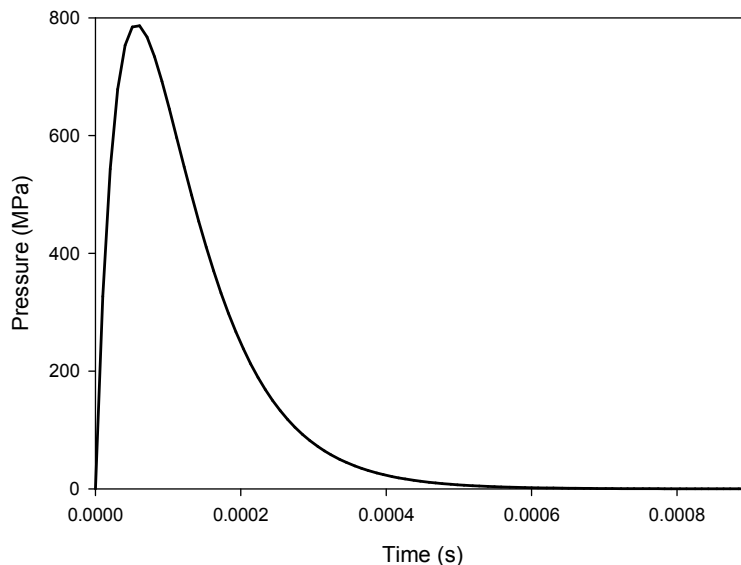


Figure 5. The input pressure pulse.

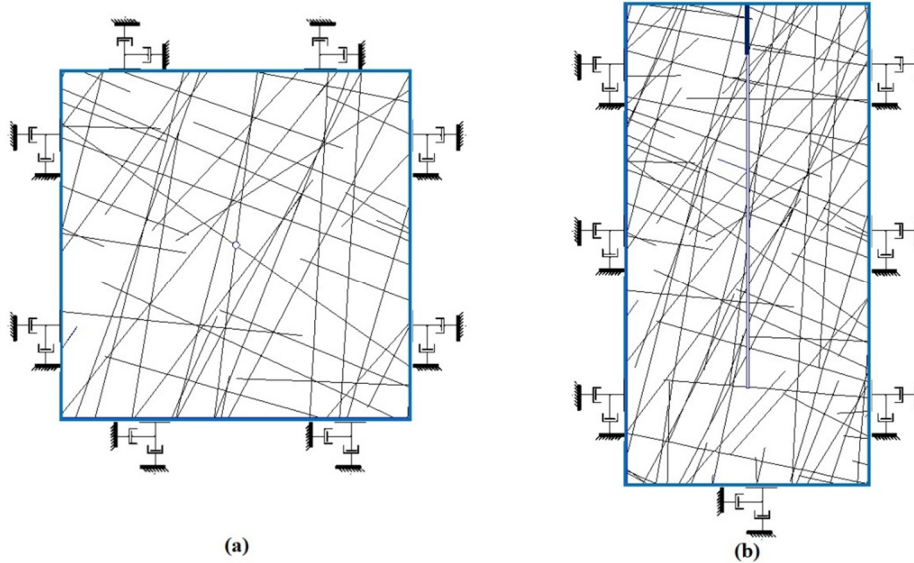


Figure 6. Dynamic boundary conditions of a) radial and b) longitudinal models.

In time-domain analyses, Rayleigh damping is commonly used to provide damping because it is approximately frequency-independent over a restricted range of frequencies [35]. Generally, the Rayleigh damping is a combination of mass-proportional and stiffness-proportional damping. The mass-proportional damping force term,  $d_i^m$ , and the stiffness-proportional damping force term,  $d_i^s$ , for translational degrees of freedom in the momentum equation take the forms:

$$d_i^m = -\gamma \frac{\partial u_i}{\partial t} m \quad (19)$$

$$d_i^s = \delta k_{ij} \frac{\partial u_i}{\partial t} \quad (20)$$

where  $m$  is the block mass or lumped mass at a grid point,  $k_{ij}$  is the contact stiffness tensor,  $\gamma$  and  $\delta$  are the mass- and stiffness-proportional constants, respectively, and  $\partial u_i / \partial t$  is the velocity in the mass-proportional damping and relative velocity at the contact in the stiffness-proportional damping [36]. Furthermore, the natural damping for geo-media is mainly hysteretic and difficult to decide but it commonly falls in a 2-5% range of critical damping [45].

## 7. Results and discussion

The two radial and longitudinal (vertical) sections of a blast hole were modeled to investigate the dynamic fracture propagation around the hole in a jointed rock mass using the dual fractured media approach. Due to the explosion in the blast hole,

the elastic waves propagate in the rock mass and transmit the explosion energy into the rock media. This energy breaks the rock into fragments due to the simultaneous fracture extension within the rock mass. In Figures 7 and 8, the velocity plot of the particles is illustrated at different times in the radial and longitudinal sections, respectively. Generally speaking, they show the shock front status in the radial and longitudinal sections of a typical exploded blast hole. It should be noted that due to the inhomogeneity and anisotropy of the jointed rock masses, the shock wave propagates accordingly.

The fracture extension process around this blast hole is shown in Figures 9 and 10. These figures demonstrate the initiation, propagation, and coalescences of radial cracks in both the radial and longitudinal sections of a blast hole.

It should be noted that Figures 9 and 10 show the situation of a completely exploded blast hole and rock fragmentation process within a millisecond.

The mechanism of dynamic fracture initiation, propagation, and coalescences around an exploded blast hole in a jointed rock mass is explained in Figures 11 (a-c). The dynamics rock fragmentation process occurred in two modes: 1) as shown in Figure 11-b, the fracture extension process may be developed from the rock mass pre-existing fractures and propagated along them 2) the cracks may be initiated and propagated in the intact rock blocks (Figure 11-c).

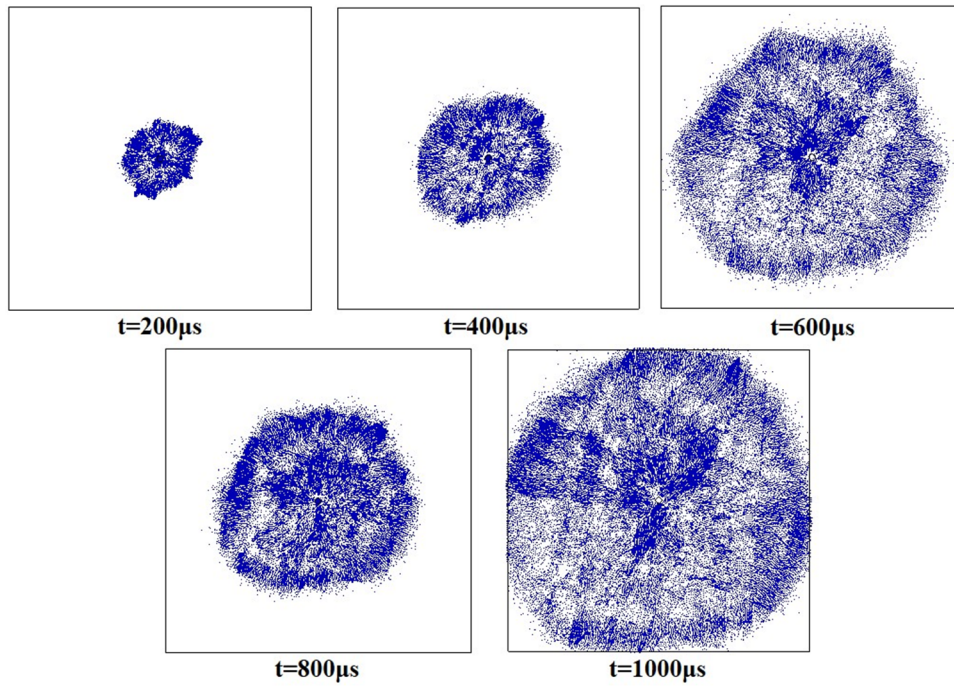


Figure 7. Shock front status of a blast hole in radial plan at different times.

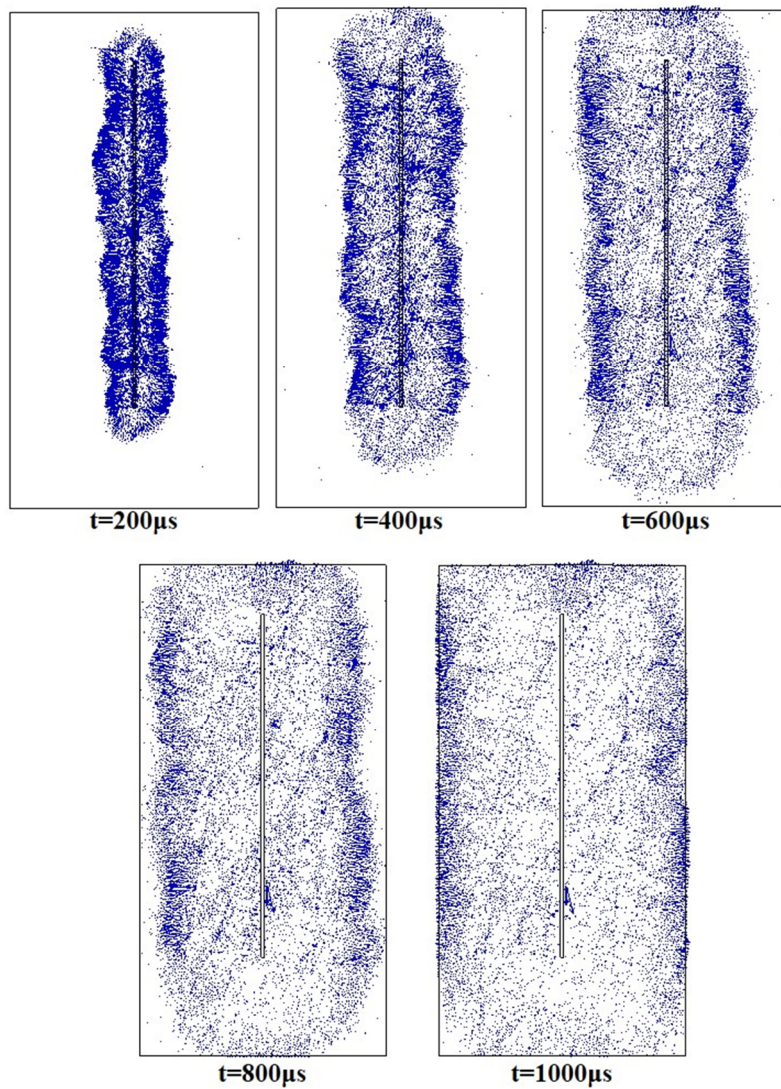


Figure 8. Shock front status in vertical (longitudinal) section of a blast hole at different times.

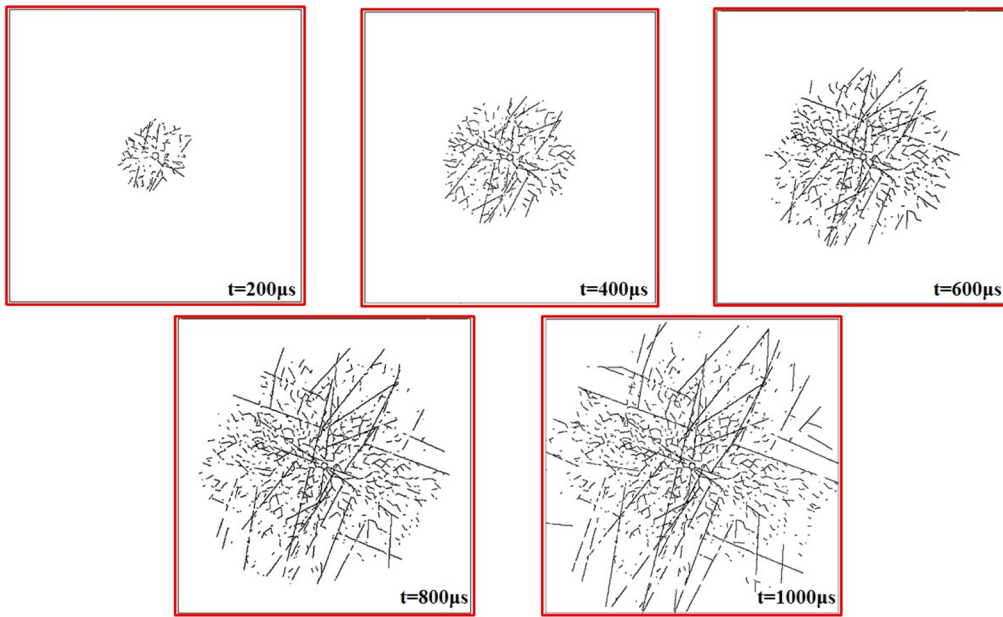


Figure 9. Fracture propagations in radial section of a blast hole at different times.

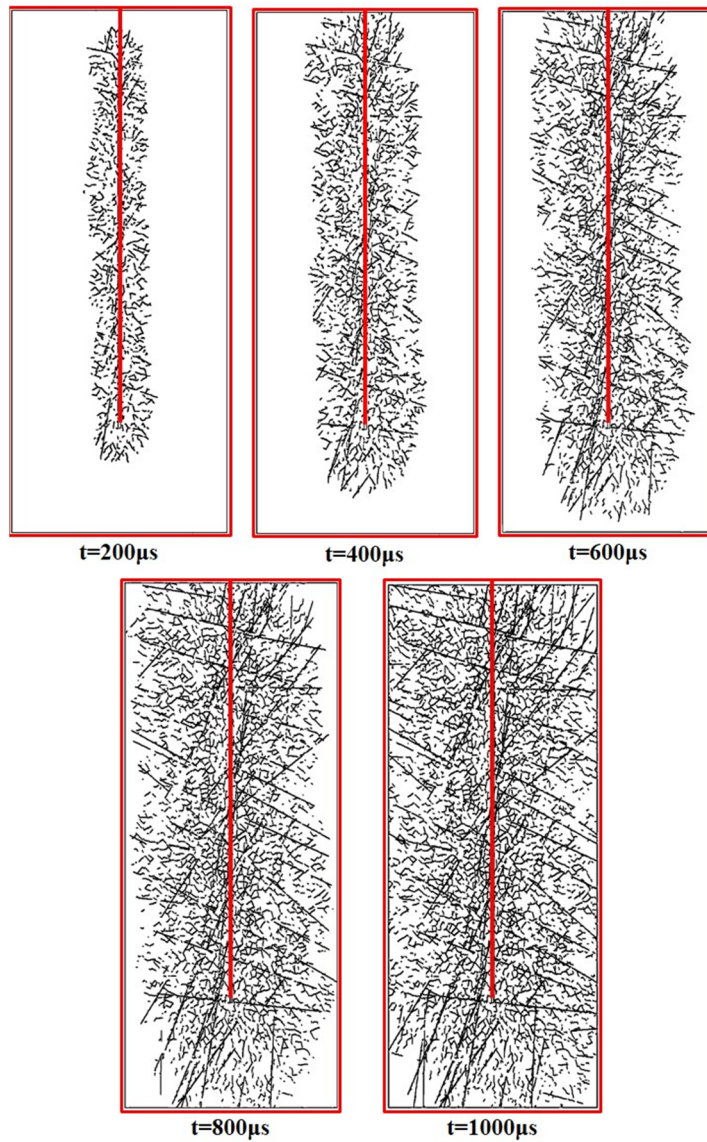


Figure 10. Fracture propagations in longitudinal section of a blast hole at different times.

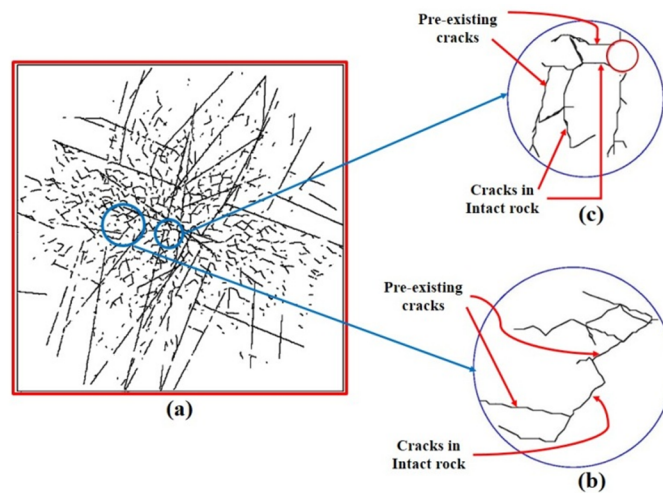


Figure 11. a) Radial section of a blast hole after explosion b) Splitting of rock mass from the pre-existing fractures c) Crack initiation and extension in the intact rock blocks d) Propagation of the pre-existing fractures from the crack tips.

### 8. Dynamic modeling of controlled blasting

To demonstrate the applicability of the proposed modeling, a typical example of a controlled exploded blast hole in a jointed rock mass was studied in this research work. In this example problem, the effect of the pre-splitting method on the fracture extension process at the back of the blast hole was numerically investigated. The over-break is an important problem at the back of the exploded area in rock slope engineering, which reduces the strength of rock mass. There are many different techniques to alleviate this destructive effect such as the pre-splitting method. This technique consists of creating a fracture plane or generally an empty area in the rock mass before firing the production blasting by means of a row of blast holes, usually of a small diameter, and with decoupled explosion charges [46].

The numerical example in this work was a typical rock slope with a 0.05 m diameter blast hole. To specify the pre-splitting effect, a 0.03 m gap was assumed as the pre-splitting gap at the back of the blast hole (Figure 12). To visualize the effect of pre-splitting, two different situations were modeled, i.e. with and without the pre-splitting gap.

The fracture patterns around the exploded blast hole (for one millisecond time duration) considering the two models (i.e. without and with pre-splitting gap models) are shown in Figures 13 and 14, respectively.

It can be visualized that the pre-splitting gap does not allow the fractures to extend at the back as well as at the explosion area (comparing Figures 13 and 14).

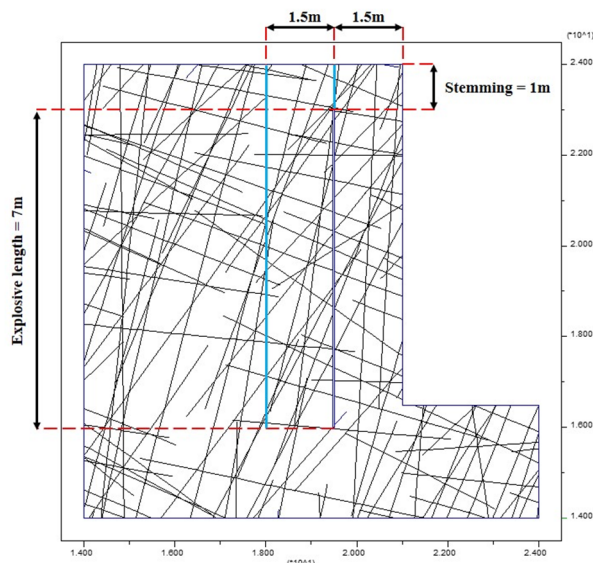


Figure 12. Numerical example geometry of a typical blast hole in a jointed rock mass.

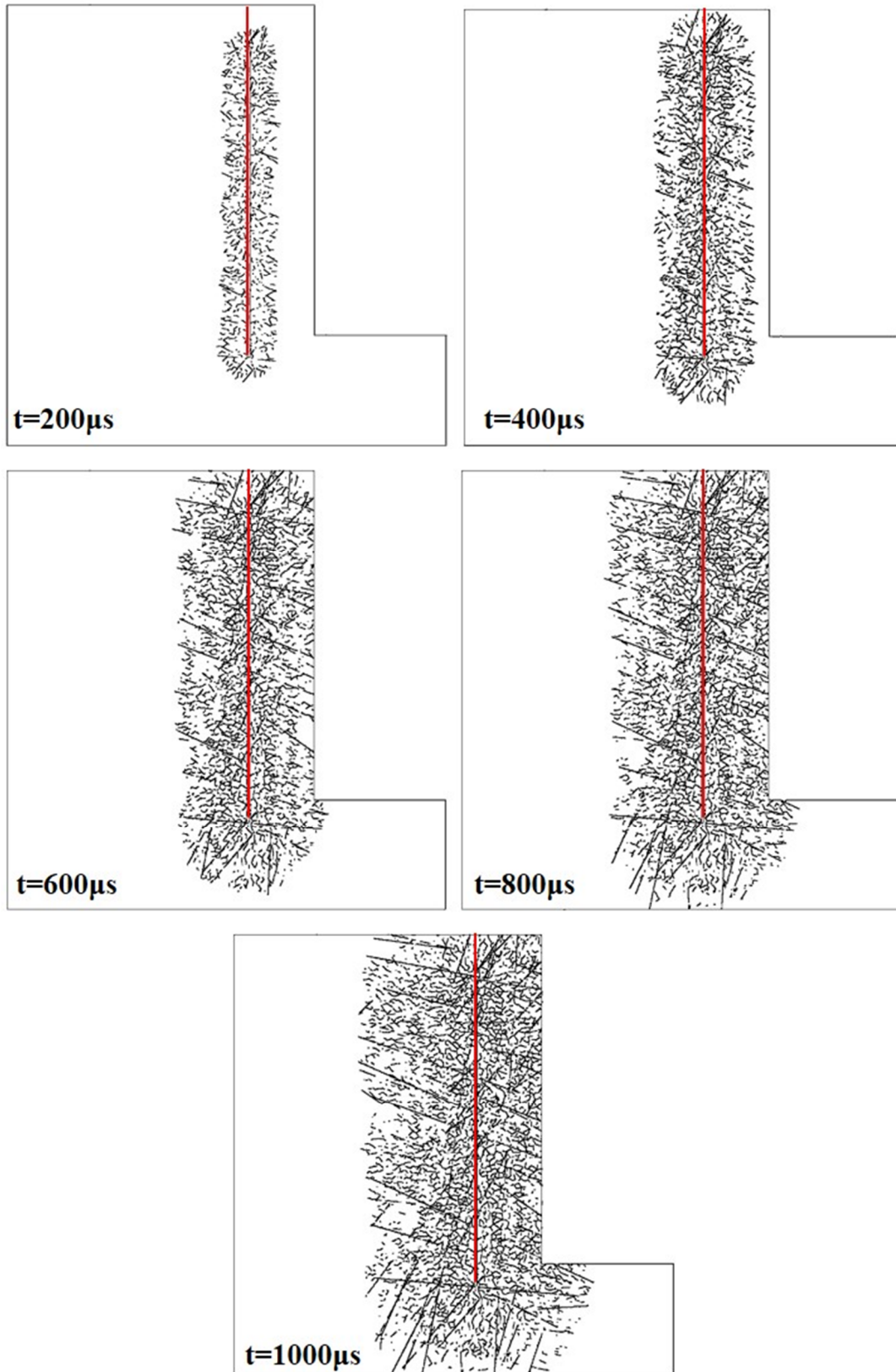


Figure 13. Fracture propagations around a blast hole (without presplitting gap model) at different times.

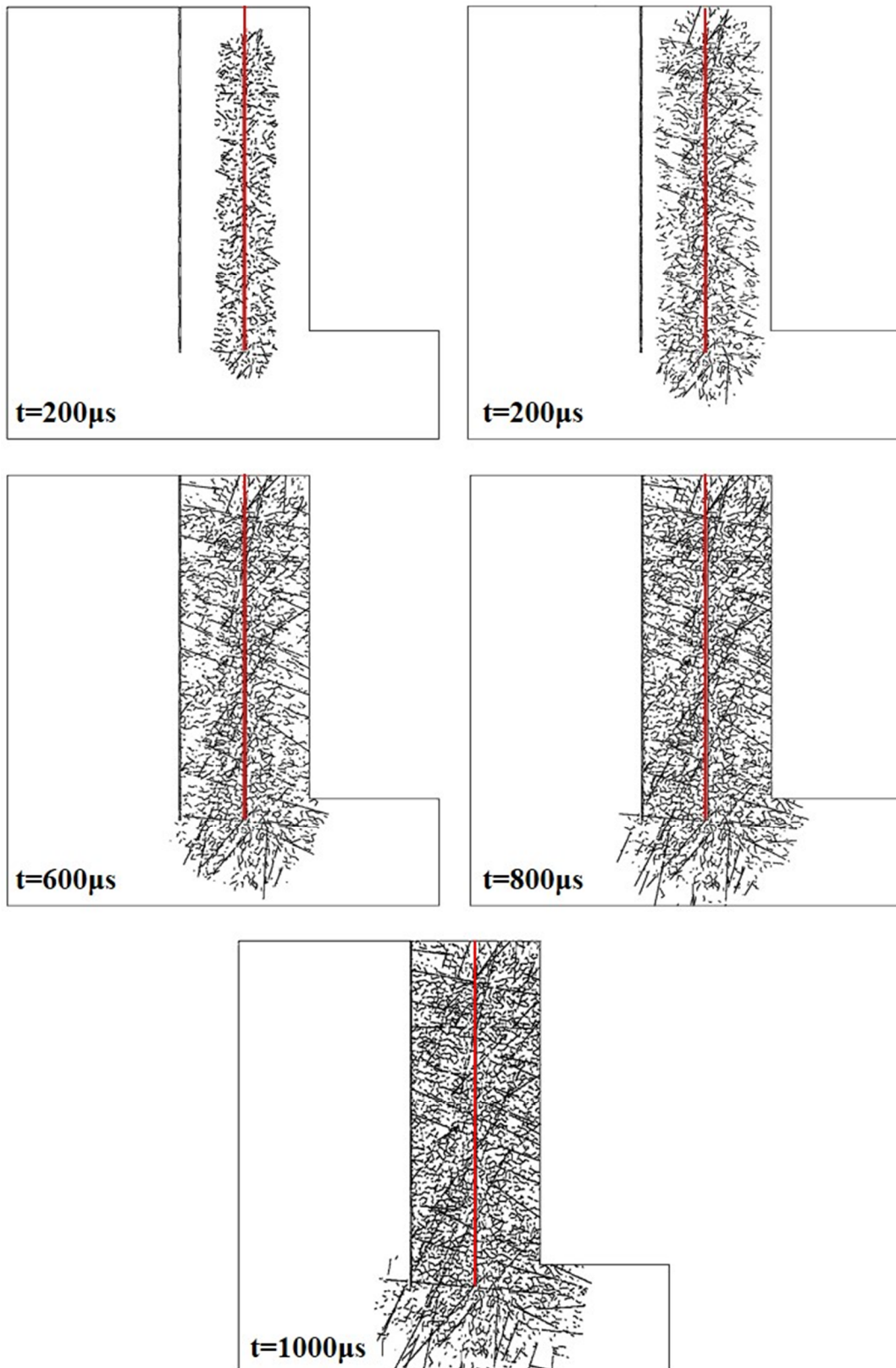


Figure 14. Fracture propagation around a blast hole (with a pre-splitting gap model) at different times.

### 9. Conclusions

The dual fracture media approach and discrete element method were utilized simultaneously to numerically model the dynamic fracture extension process in a jointed rock mass around an exploded

blast hole. An explosion occurs in two stages: shock wave propagation and gas extension. In this work, the blast-induced shock wave was considered as the dynamic input pulse.

The DFN approach and Voronoi technique were used to generate the pre-existing rock fractures and newly cracks in the intact rock, respectively. This research work demonstrates that the proposed modeling procedure may be capable of simulating the rock blasting problems related to fracture propagation in a jointed rock mass considering both the pre-existing fractures and the newly created cracks in the intact rock. Therefore, crack initiation and propagation in the intact rock around the blast hole can also occur. It may be concluded that the dynamic fracture extension process can be accomplished in two modes: 1) the new cracks may be initiated and extended dynamically in the intact rock blocks 2) the dynamic fracture extension may be developed from the rock mass pre-existing fractures. The applicability of the present method was represented by modeling a typical example problem numerically. The dynamic fracture extension patterns of this example problem indicated that the new and inherent cracks just extended in front of the pre-splitting gap, and its back area was not affected. This example illustrates that the deployed procedure is capable of modeling the explosion process in controlled blasting methods and can be utilized for different fracture propagations and fragmentation processes in the rock masses.

## References

- [1]. Bhandari, S. (1979). On the role of stress waves and quasi-static gas pressure in rock fragmentation by blasting. *Acta Astronautica*. 6: 365-383.
- [2]. Dowding, C.H. and Aimone, C.T. (1985). Multiple blast-hole stresses and measured fragmentation. *Rock Mechanics and Rock Engineering*. 18: 17-36.
- [3]. Zhang, Y.Q., Hao, H. and Lu, Y. (2003). Anisotropic dynamic damage and fragmentation of rock materials under explosive loading. *International Journal of Engineering Science*. 41: 917-929.
- [4]. Dehghan Banadaki, M.M. (2010). Stress-wave induced fracture in rock due to explosive action, PhD thesis, University of Toronto, Canada.
- [5]. Dehghan Banadaki, M.M. and Mohanty, B. (2012). Numerical simulation of stress wave induced fractures in rock. *International Journal of Impact Engineering*. 40-41: 16-25.
- [6]. Fatehi Marji, M. (1997). Modeling of cracks in rock fragmentation with a higher order displacement discontinuity method, PhD thesis, Middle East Technical University (METU), Turkey.
- [7]. Fatehi Marji, M., Goshtasbi, K., Gholamnejad, J. and Haeri, H. (2010). On the displacement discontinuity analysis of radial cracks emanating from circular blast holes in rock blasting, ISRM International and 6<sup>th</sup> Asian Rock Mechanics Symposium, New Delhi, India.
- [8]. Hosseini Nasab, H. and Fatehi Marji, M. (2007). A semi-infinite higher order displacement discontinuity method and its application to the quasi-static analysis of radial cracks produced by blasting. *Journal of Mechanics of Material and Structures*. 2 (3): 439-458.
- [9]. Cho, S.H. and Kaneko, K. (2004). Influence of the applied pressure waveform on the dynamic fracture processes in rock. *International Journal of Rock Mechanics and Mining Sciences*. 41: 771-784.
- [10]. Chun-Rui, L., Li-jun, K., Qing-xing, Q., De-bing, M., Quan-ming, L. and Gang, X. (2009). The numerical analysis of borehole blasting and application in coal mine roof-weaken. *Procedia Earth and Planetary Science*. 1: 451-459.
- [11]. Saharan, M.R. and Mitri, H.S. (2008). Numerical procedure for dynamic simulation of discrete fractures due to blasting. *Rock Mechanics and Rock Engineering*. 41 (5): 641-670.
- [12]. Zhu, Z., Mohanty, B. and Xie, H. (2007). Numerical investigation of blasting-induced crack initiation and propagation in rocks. *International Journal of Rock Mechanics and Mining Sciences*. 44: 412-424.
- [13]. Lak, M., Fatehi Marji, M., Yarahmadi Bafghi, A. and Abdollahipour, A. (2018). Numerical modelling of crack initiation around a wellbore due to explosion. *International Journal of Geological and Environmental Engineering*. 12 (6): 395-398.
- [14]. Munjiza, A., Owen, D.J. and Bicanic, N. (1995). A combined finite-discrete element method in transient dynamics of fracturing solids. *Engineering Computations*. 12 (2): 145-174.
- [15]. Ning, Y., Yang, J., An, X. and Ma, G. (2011). Modelling rock fracturing and blast-induced rock mass failure via advanced discretisation within the discontinuous deformation analysis framework. *Computers and Geotechnics*. 38: 40-49.
- [16]. Onederra, I.A., Furtney, J.K., Sellers, E. and Iverson, S. (2013). Modelling blast induced damage from a fully coupled explosive charge. *International Journal of Rock Mechanics and Mining Sciences*. 58: 73-84.
- [17]. Bendezu, M., Romanel, C. and Roehl, D. (2017). Finite element analysis of blast-induced fracture propagation in hard rocks. *Computers and Structures*. 182: 1-13.
- [18]. Jian-sheng, T. and Fan-Fei, Q. (2009). Model experiment of rock blasting with single borehole and double free-surface. *Mining Science and Technology*. 19: 395-398.

- [19]. Ma, G.W. and An, X.M. (2008). Numerical simulation of blasting-induced rock fractures. *International Journal of Rock Mechanics and Mining Sciences*. 45: 966-975.
- [20]. Wang, Z.L. and Konietzky, H. (2009). Modelling of blast-induced fractures in jointed rock masses. *Engineering Fracture Mechanics*. 76: 1945-1955.
- [21]. Trivino, L.F. (2012). Study of blast-induced damage in rock with potential application to open pit and underground mines, PhD thesis, University of Toronto, Toronto, Canada.
- [22]. Trivino, L.F. and Mohanty, B. (2015). Assessment of crack initiation and propagation in rock from explosion-induced stress waves and gas expansion by cross-hole seismometry and FEM-DEM method. *International Journal of Rock Mechanics and Mining Sciences*. 77: 287-299.
- [23]. Duvall, W.I. (1953). Strain-wave shapes in rock near explosions. *Geophysics*. 18: 310-323.
- [24]. Favreau, R.F. (1969). Generation of strain waves in rock by an explosion in a spherical cavity. *Journal of Geophysical Research*. 74 (17): 4267-4280.
- [25]. Chen, S.G. and Zhao, J. (1998). A study of UDEC modelling for blast wave propagation in jointed rock masses. *International Journal of Rock Mechanics and Mining Sciences*. 35 (1): 93-99.
- [26]. Chen, S.G., Cai, J.G., Zhao, J. and Zhou, Y.X. (2000). Discrete element modelling of an underground explosion in a jointed rock mass. *Geotechnical and Geological Engineering*. 18: 59-78.
- [27]. Starfield, A.M. and Pugliese, J.M. (1968). Compression waves generated in rock by cylindrical explosive charges: a comparison between a computer model and field measurements. *International Journal of Rock Mechanics and Mining Sciences*. 5: 65-77.
- [28]. Kipp, M.E., Grady, D.E. and Chen, E.P. (1980). Strain rate dependent fracture initiation. *International Journal of Fracture*. 16: 471-478.
- [29]. Whittaker, B.N., Singh, R.N. and Sun, G. (1992). *Rock Fracture Mechanics*, Elsevier Science, Amsterdam.
- [30]. Hu, R., Zhu, Z., Xie, J. and Xiao, D. (2015). Numerical study on crack propagation by using softening model under blasting. *Advances in Materials Science and Engineering*. doi:10.1155/2015/108580.
- [31]. Aliabadian, Z., Sharafisafa, M., Mortazavi, A. and Maarefvand, P. (2014). Wave and fracture propagation in continuum and faulted rock masses: distinct element modeling. *Arabian Journal of Geoscience*. 7: 5021-5035.
- [32]. Habibi, M.J., Mokhtari, A.R., Baghbanan, A. and Namdari, S. (2014). Prediction of permeability in dual fracture media by multivariate regression analysis. *Journal of Petroleum Science and Engineering*. 120: 194-201.
- [33]. Zhang, X., Sanderson, D.J. and Barker, A.J. (2002). Numerical study of fluid flow of deforming fractured rocks using dual permeability model. *Geophysical Journal International*. 151: 452-468.
- [34]. Cundall, P.A. and Hart, R.D. (1993). Numerical Modeling of Discontinua- *Comprehensive Rock Engineering*. In: Hudson, J.A. (Ed.). *Comprehensive Rock Engineering*. 1<sup>st</sup> Edition, Pergamon Press. 2: 231-244.
- [35]. Itasca Consulting Group, Inc. (2000). (UDEC) Universal Distinct Element Code (Version 3.1) User's Guide, Minneapolis, Minnesota.
- [36]. Jing, L. and Stephansson, O. (2007). *Fundamentals of Discrete Element Methods*, Elsevier.
- [37]. Bui, T.T., Limam, A., Sarhosis, V. and Hjiat, M. (2017). Discrete element modelling of the in-plane and out-of-plane behavior of dry-joint masonry wall constructions. *Engineering Structures*. 136: 277-294.
- [38]. EBE German consulting engineers Co. (2007). Rock mechanics laboratory report on borehole No. 6A, Choghart iron mine reports archive.
- [39]. Bhandari, S. (1997). *Engineering Rock Blasting Operations*, A. A. Balkema, Rotterdam.
- [40]. Lopez Jimeno, C., Lopez Jimeno, E. and Carcedo, F.J. (1995). *Drilling and Blasting of Rocks*, Balkema, Rotterdam.
- [41]. Sharpe, J.A. (1942). The production of elastic waves by explosion pressures. *Geophysics*. 7: 144-154.
- [42]. Brady, B.H.G. and Brown, E.T. (2005). *Rock Mechanics for underground mining*, 3<sup>rd</sup> Edition, Springer.
- [43]. Lysmer, J. and Kuhlemeyer, R.L. (1969). Finite Dynamic Model for Infinite Media. *Journal of Engineering Mechanics Division*. 95: 859-878.
- [44]. Lak, M., Baghbanan, A. and Hashemolhoseini, H. (2017). Effect of seismic waves on the hydro-mechanical properties of fractured rock masses. *Earthquake Engineering and Engineering Vibration*. 16 (3): 525-536.
- [45]. Cundall, P.A. (1990). Numerical Modelling of Jointed and Faulted Rock. In: Rossmanith, H.P. (Ed.). *Mechanics of Jointed and Faulted Rock*. A. A. Balkema, Rotterdam.
- [46]. Hustrulid, W.A. and Johnson J. (2008). A Gas Pressure-based Drift Round Blast Design Methodology. 5<sup>th</sup> International Conference and Exhibition on Mass Mining, Sweden, Lulea, Lulea University of Technology. pp. 657-669.

## مدل‌سازی المان مجزای گسترش شکستگی ناشی از انفجار در توده‌سنگ درزه‌دار

میثم لک<sup>۱</sup>، محمد فاتحی مرجی<sup>۱\*</sup>، علیرضا یاراحمدی<sup>۱</sup> و ابوالفضل عبدالهی پور<sup>۲</sup>

۱- دانشکده مهندسی معدن و متالورژی، دانشگاه یزد، ایران

۲- پژوهشگاه صنعت نفت، گروه پژوهش و فناوری‌های حفاری و تکمیل چاه، تهران، ایران

ارسال ۲۰۱۸/۷/۲۳، پذیرش ۲۰۱۸/۱۱/۲۹

\* نویسنده مسئول مکاتبات: mfatehi@yazd.ac.ir

---

### چکیده:

فرآیند انفجار مواد منفجره در یک چال، فشار بسیار زیادی را به محیط سنگی اطراف خود وارد می‌کند. این روند ممکن است باعث شروع و گسترش درزه در سنگ و در نهایت باعث خردایش سنگ شود. خردایش سنگ بر اثر انفجار، عمدتاً بر اثر گسترش ترک‌های موجود در سنگ و همچنین ایجاد و توسعه ترک‌های جدید ایجاد می‌شود. در این مطالعه، فرآیند گسترش ترک‌های ناشی از انفجار در توده‌سنگ به روش المان مجزا شبیه‌سازی شده است. لازم به ذکر است که در این مطالعه، انتشار شکستگی‌ها از هر دو مورد شکستگی‌های موجود و ترک‌های جدید ایجاد شده در نظر گرفته شده است. شکستگی‌های ذاتی توده‌سنگ با استفاده از تکنیک شبکه شکستگی مجزا ایجاد شده‌اند. به منظور فراهم کردن امکان توسعه شکستگی‌ها در بلوک‌های سنگ بکر، این بلوک‌ها توسط تکنیک Voronoi به بلوک‌های ثانویه تقسیم شده‌اند. پس از اتمام مدل‌سازی، فرآیند توسعه شکستگی در مقاطع شعاعی و طولی از چال انفجاری مشخص شده است. سپس یک چال انفجاری در یک شیروانی سنگی فرضی مدل شده است و اثر روش پیش شکافی (انفجار کنترل شده) در ناحیه پشت چال انفجاری بر فرآیند توسعه شکستگی در ناحیه انفجاری به عنوان یک کاربرد از روش ارائه شده، مورد بررسی قرار گرفته است. نتایج حاصل از مدل‌سازی نشان می‌دهد که روند ارائه شده قادر به مدل‌سازی فرآیند انفجار و فرآیندهای مختلف انتشار شکستگی‌ها و خردایش سنگ مانند انفجار کنترل شده است.

**کلمات کلیدی:** انفجار توده‌سنگ، شکست دینامیکی، گسترش ترک، روش المان مجزا، شبکه شکستگی مجزا.

---